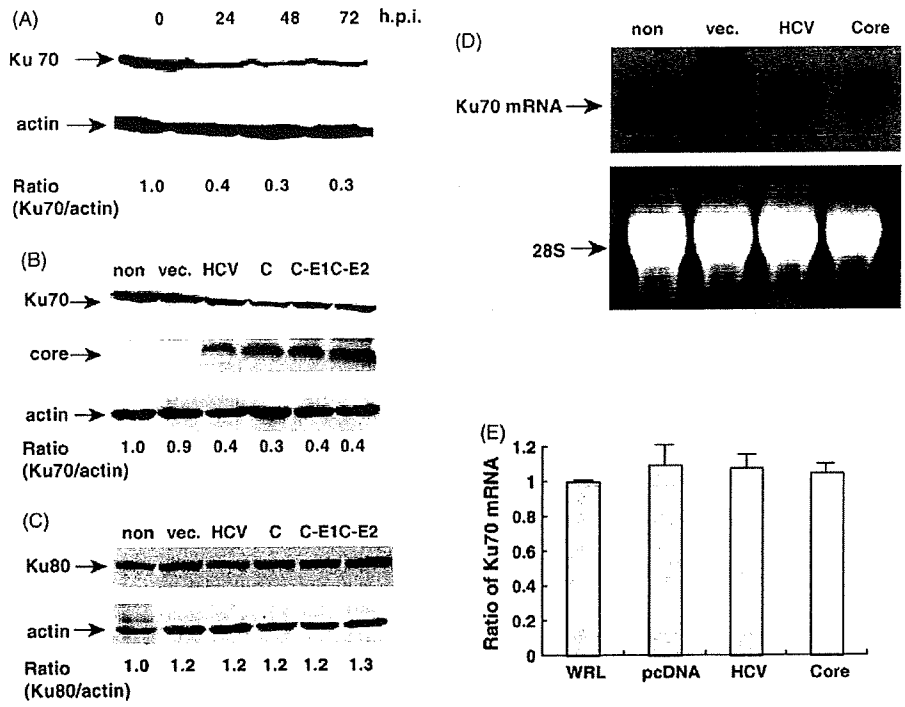

Fig. 3. Effects of HCV on the Ku70 and Ku80 expression levels. (A) The levels of Ku70 protein in WRL68 cells at 0, 24, 48, and 72 h after transfection with the full-length HCV genome (pCA-Rz plasmid) were determined by Western blotting. The band intensities were analyzed by densitometry, normalized by actin, and the expression ratio was determined by division with the level at 0 h (A) or non(B and C). Levels of Ku70 (B) and Ku80 (C) in WRL68 cells that express the pcDNA vector (vec), full-length HCV genome (HCV), HCV-core protein sequence (Core), HCV core plus E1 sequence (c-E1), or the HCV core plus the E1 and E2 sequences (c-E2). Cells were lyzed 48 h after transfection. Representative data from three experiments are presented. (D) Ku70 mRNA levels in WRL68 cells transfected with the mock (non), pcDNA vector (vec), full-length HCV genome (HCV) or the HCV-core protein sequence (Core), as assessed in an autoradiographic image of the Northern blot (upper). The 28S rRNA was detected by ethidium bromide staining (lower). (E) The mRNA bands were analyzed by densitometry, normalized by the 28S rRNA band, and the expression ratio was calculated by dividing the intensity of the each band by the intensity of the band for the mock-transfected WRL68 cells (WRL). The average values from three experiments are presented; vertical bars, S.D.

identify the protein encoded by the HCV genome that is responsible for this effect, we transfected the truncated *HCR6-Rz* DNA into WRL68 cells (Fig. 3B). After 48 h, Ku70 expression was suppressed by the full-length or truncated HCV genome, and especially by the HCV-core protein sequence (Fig. 3B).

Since the Ku70 antigen, Ku80 antigen, and DNA-PK$_{cs}$ compose DNA-PK, we also examined the effect of transfection with the HCV genome on the level of Ku80 (Fig. 3C). Transfection with the full-length HCV genome did not significantly influence the level of Ku80 (Fig. 3C). In addition, Western blotting showed that the level of HCV-core protein was lower in cells that were transfected with the full-length HCV genome than in those transfected with truncated HCV genomes, with similar levels of suppression of Ku70 expression being noted (Fig. 3B), which indicates that certain amount of HCV-core protein expression may be sufficient for the suppression of Ku70.

To determine the mechanism by which HCV reduces the level of Ku70 in WRL68 cells, we examined the effects of transfection with the HCV genome and HCV core on the transcription of Ku70 mRNA using Northern blotting (Fig. 3D). Transfection with the HCV genome and HCV core did not cause significant changes in the levels of Ku70 mRNA (Fig. 3E).

3.4. Kinetics of Ku70 degradation in the presence of HCV proteins

As our results indicated that changes in transcription do not account for the changes in the levels of Ku70, we investigated the possibility that these changes were due to alterations in the stability of the Ku70 protein. WRL68 cells were transfected with the full-length HCV genome or the sequence that encodes the HCV-core protein, and thereafter the cells were allowed to accumulate Ku70. Protein synthesis was then blocked by treating the cells with cycloheximide, and the degradation of Ku70 was monitored by protein quantitation using Western blotting (Fig. 4A and B). We found that the degradation of Ku70 occurred significantly faster in cells that expressed the HCV-core protein or the full-length HCV genome than in non-transfected cells.

These results reveal that expression of the full-length HCV genome or the HCV-core protein sequence significantly reduces the stability of Ku70 in WRL68 cells. Therefore, we examined whether this was due to the changes in the ubiquitin–proteasome system. Ku70 was immunoprecipitated from cell lysates and analyzed by Western blotting using an anti-ubiquitin antibody. We found that the ubiquitination of Ku70 was significantly enhanced in WRL68 cells by the expression of either the full-length HCV genome or the HCV-core protein sequence (Fig. 4C). Therefore, it appears that the ubiquitin–proteasome system for Ku70 is activated by the expression of the full-length HCV genome or the HCV-core protein.

3.5. Kinetics of DNA-PK activity in the presence of HCV proteins

Since Ku70 is a component of DNA-PK, we examined the effect of HCV on the activity of DNA-PK. Following the transfection of WRL68 cells with the full-length HCV genome for 48 h, DNA-PK$_{cs}$ was immunoprecipitated with a rabbit polyclonal antibody, and the protein kinase activity was assessed using a substrate peptide derived from p53. We found that the protein kinase activity of DNA-PK$_{cs}$ was approximately 20% lower in HCV-transfected cells than in the vector DNA-transfected cells (Fig. 5A). Furthermore, Ku70

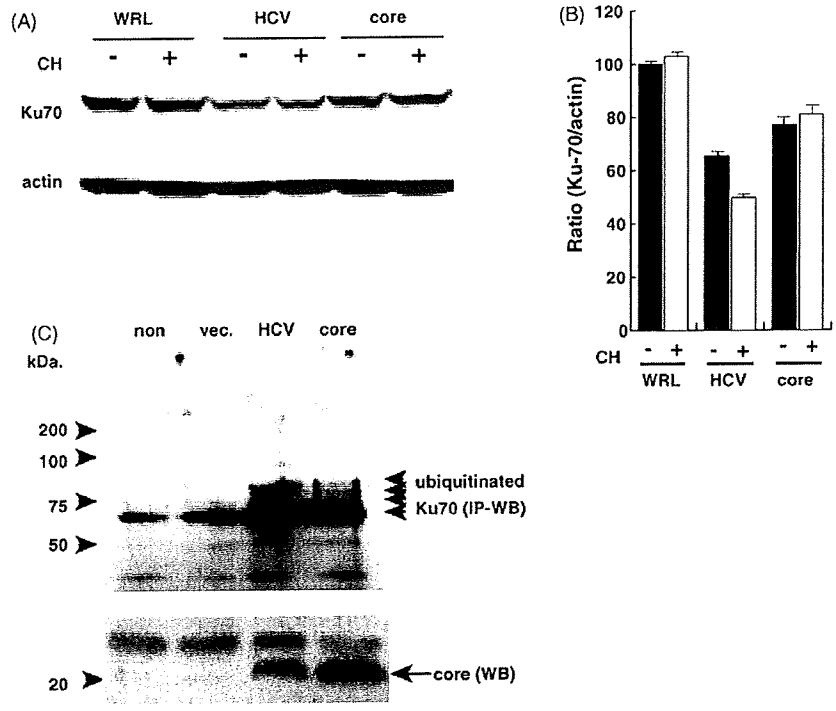

Fig. 4. Ku70 degradation kinetics in the presence of HCV-core protein. (A) WRL68 cells were transfected with the full-length HCV genome (HCV) using the pCA-Rz plasmid, the HCV-core sequence (Core) or mock (WRL) for 24 h, treated with cycloheximide (CH) to block *de novo* protein synthesis, and analyzed by Western blotting after 0 h (–) and 0.5 h (+). (B) Ku70 was quantified by densitometry, and the expression ratio was determined by actin normalization and division by the intensity value for mock (WRL) at 0 h. The average values for three experiments are indicated; vertical bars, S.D. (C) Ubiquitination of Ku70 was examined by immunoprecipitation–Western blotting in cells transfected with the mock (non), pcDNA vector (vec), HCV, and HCV core sequence (upper). The HCV-core protein was detected in these cells (lower).

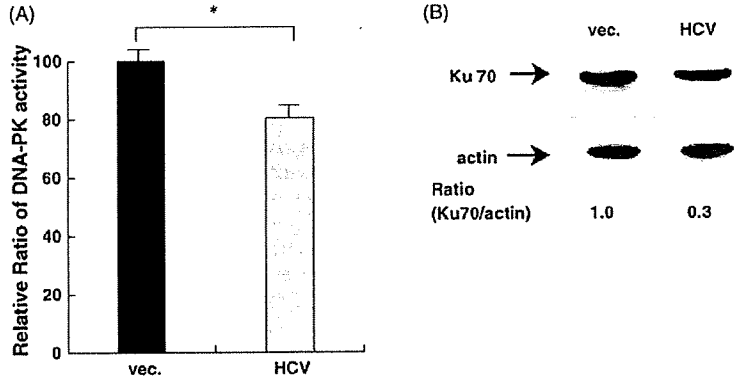

Fig. 5. Modification of DNA-PK activity by HCV. (A) DNA-PK activity was detected by the immunoprecipitation-kinase assay, and the extent of phosphorylation was determined by autoradiography after 48 h of plasmid DNA transfection. The relative ratio of DNA-PK activity was determined by normalizing the activity by the activity detected in the vector DNA-transfected WRL68 cells (WRL). The average values of three experiments are presented; vertical bars, S.D. (B) The levels of Ku70 protein and actin in cells were measured by Western blotting after 48 h of plasmid DNA transfection.

expression was significantly reduced in the HCV-expressing cells (Fig. 5B).

4. Discussion

In the present study, we show that HCV, and in particular the HCV-core protein, promotes the ubiquitination of Ku70 in the human embryonic liver cell line WRL68. This phenomenon was not observed following the transfection or infection of HCV into hepatoma-derived cell lines (data not shown). These HCV proteins may reduce Ku70 expression in the noncancerous liver tissues of the majority of HCV-infected patients. It has been reported that HCV levels are significantly higher in noncancerous tissues than in cancerous tissues ($p < 0.001$) (Tanaka et al., 2004; Young et al., 2002). Therefore, the reduction in the level of Ku70 might be expected to be more pronounced in HCV-positive noncancerous liver tissues than in either cancerous liver tissues or the liver tissues of HCV-negative HCC patients. The lack of consistency observed in the Ku70 expression profiles of the HCV-negative HCC patients suggests that Ku70 may play a less prominent role in these patients than it does in HCV-positive HCC patients.

Ku binds to DNA ends and targets DNA-PK_{cs} to DNA strand breaks (Gottlieb and Jackson, 1993; Suwa et al., 1994). Ku70 and Ku80 are the DNA-binding components of DNA-PK (Anderson and Carter, 1996; Anderson and Lees-Miller, 1992; Dynan and Yoo, 1998) and

play roles in a variety of nuclear functions, including transcriptional regulation, V(D)J recombination, and a specific DNA repair mechanism called nonhomologous end-joining (Koike, 2002; Lombard et al., 2005). DNA-PK activity is associated with chromosomal instability and in peripheral blood lymphocytes of patients at risk for breast and cervical cancer (Someya et al., 2006). A study using reverse transcription-PCR showed that the expression levels of Ku70, Ku86, and DNA-PK_{cs} are interrelated (Someya et al., 2006). In general, the expression levels of DNA-PK_{cs} and Ku80 are up-regulated in malignant tumors in human tissues, with the exception of invasive carcinoma of the breast (Moll et al., 1999). Marked reductions in the expression levels of Ku70 and Ku80 beginning at the adenoma stage may be crucial for the development of colon cancer (Rigas et al., 2001). A separate study showed that DNA-PK activates p53 in response to DNA damage, allowing p53 to bind to specific DNA sequences and preventing MDM2 from inhibiting p53-dependent transactivation (Woo et al., 1998). The results of the present study suggest that HCV-induced reductions of Ku70 expression and DNA-PK activity decrease the ability of the cell to protect the genome against environmental insults, resulting in genomic instability and HCC.

Recently, Ku70 was identified as a mammalian receptor for *Rickettsia conorii*. Infection with *R. conorii* stimulates the ubiquitination of Ku70, which may contribute to bacterial invasion (Martinez et al., 2005). Further studies regarding the possibility that Ku70 degradation by HCV-core protein is linked to the HCV entry process are warranted.

In summary, the results of the present study reveal a novel function of the HCV-core protein in noncancerous liver cells, whereby it facilitates the degradation of Ku70 and reduces DNA-PK activity. These properties of the HCV-core protein may reveal the molecular basis of hepatocarcinogenesis induced by HCV in normal liver cells.

Acknowledgments

We thank Michinori Kohara for generously supplying plasmids, cell lines, and antibodies (MoAb 31-2), Shinobu Ohmi and Hiroyuki Fukuda for performing MALDI-TOF-MS, Makoto Saito for critical comments, and Nobuaki Funada and Takeshi Tanaka for supplying patients' tissues. This work was supported by grants from the Ministry of Health and Welfare and the Ministry of Education, Culture, Sports, Science and Technology of Japan, the Program for the Promotion of Fundamental Studies in Health Sciences of the National Institute of Biomedical Innovation, and the Cooperative Research Project on Clinical and Epidemiological Studies of Emerging and Re-emerging Infectious Diseases.

References

Anderson, C.W., Carter, T.H., 1996. The DNA-activated protein kinase—DNA-PK. Curr. Top. Microbiol. Immunol. 217, 91–111.
Anderson, C.W., Lees-Miller, S.P., 1992. The nuclear serine/threonine protein kinase DNA-PK. Crit. Rev. Eukaryot. Gene Expr. 2 (4), 283–314.
Baek, K.H., Park, H.Y., Kang, C.M., Kim, S.J., Jeong, S.J., Hong, E.K., Park, J.W., Sung, Y.C., Suzuki, T., Kim, C.M., Lee, C.W., 2006. Overexpression of hepatitis C virus NS5A protein induces chromosome instability via mitotic cell cycle dysregulation. J. Mol. Biol. 359 (1), 22–34.
Chang, J., Yang, S.H., Cho, Y.G., Hwang, S.B., Hahn, Y.S., Sung, Y.C., 1998. Hepatitis C virus core from two different genotypes has an oncogenic potential but is not sufficient for transforming primary rat embryo fibroblasts in cooperation with the H-ras oncogene. J. Virol. 72 (4), 3060–3065.
Collier, J.D., Bassendine, M.F., Burt, A.D., Major, G.N., 1996. Characterisation of the DNA repair enzyme for O(6)-methylguanine in cirrhosis. J. Hepatol. 25 (2), 158–165.
Dynan, W.S., Yoo, S., 1998. Interaction of Ku protein and DNA-dependent protein kinase catalytic subunit with nucleic acids. Nucleic Acids Res. 26 (7), 1551–1559.
Feit, C., Bartal, A.H., Tauber, G., Dymbort, G., Hirshaut, Y., 1983. An enzyme-linked immunosorbent assay (ELISA) for the detection of monoclonal antibodies recognizing surface antigens expressed on viable cells. J. Immunol. Methods 58 (3), 301–308.
Gottlieb, T.M., Jackson, S.P., 1993. The DNA-dependent protein kinase: requirement for DNA ends and association with Ku antigen. Cell 72 (1), 131–142.
Jensen, O.N., Wilm, M., Shevchenko, A., Mann, M., 1999. Sample preparation methods for mass spectrometric peptide mapping directly from 2-DE gels. Methods Mol. Biol. 112, 513–530.
Kohler, G., Milstein, C., 1975. Continuous cultures of fused cells secreting antibody of predefined specificity. Nature 256 (5517), 495–497.
Koike, M., 2002. Dimerization, translocation and localization of Ku70 and Ku80 proteins. J. Radiat. Res. (Tokyo) 43 (3), 223–236.
Lehrach, H., Diamond, D., Wozney, J.M., Boedtker, H., 1977. RNA molecular weight determinations by gel electrophoresis under denaturing conditions, a critical reexamination. Biochemistry 16 (21), 4743–4751.
Lengauer, C., Kinzler, K.W., Vogelstein, B., 1998. Genetic instabilities in human cancers. Nature 396 (6712), 643–649.
Lombard, D.B., Chua, K.F., Mostoslavsky, R., Franco, S., Gostissa, M., Alt, F.W., 2005. DNA repair, genome stability, and aging. Cell 120 (4), 497–512.
Machida, K., Cheng, K.T., Pavio, N., Sung, V.M., Lai, M.M., 2005. Hepatitis C virus E2-CD81 interaction induces hypermutation of the immunoglobulin gene in B cells. J. Virol. 79 (13), 8079–8089.
Martinez, J.J., Seveau, S., Veiga, E., Matsuyama, S., Cossart, P., 2005. Ku70, a component of DNA-dependent protein kinase, is a mammalian receptor for *Rickettsia conorii*. Cell 123 (6), 1013–1023.
Moll, U., Lau, R., Sypes, M.A., Gupta, M.M., Anderson, C.W., 1999. DNA-PK, the DNA-activated protein kinase, is differentially expressed in normal and malignant human tissues. Oncogene 18 (20), 3114–3126.
Moriya, K., Fujie, H., Shintani, Y., Yotsuyanagi, H., Tsutsumi, T., Ishibashi, K., Matsuura, Y., Kimura, S., Miyamura, T., Koike, K., 1998. The core protein of hepatitis C virus induces hepatocellular carcinoma in transgenic mice. Nat. Med. 4 (9), 1065–1067.
Ray, R.B., Lagging, L.M., Meyer, K., Ray, R., 1996. Hepatitis C virus core protein cooperates with ras and transforms primary rat embryo fibroblasts to tumorigenic phenotype. J. Virol. 70 (7), 4438–4443.
Rigas, B., Borgo, S., Elhosseiny, A., Balatsos, V., Manika, Z., Shinya, H., Kurihara, N., Go, M., Lipkin, M., 2001. Decreased expression of DNA-dependent protein kinase, a DNA repair protein, during human colon carcinogenesis. Cancer Res. 61 (23), 8381–8384.
Saito, I., Miyamura, T., Ohbayashi, A., Harada, H., Katayama, T., Kikuchi, S., Watanabe, Y., Koi, S., Onji, M., Ohta, Y., et al., 1990. Hepatitis C virus infection is associated with the development of hepatocellular carcinoma. Proc. Natl. Acad. Sci. U.S.A. 87 (17), 6547–6549.
Smirnova, I.S., Aksenov, N.D., Kashuba, E.V., Payakurel, P., Grabovetsky, V.V., Zaberezhny, A.D., Vonsky, M.S., Buchinska, L., Biberfeld, P., Hinkula, J., Isaguliants, M.G., 2006. Hepatitis C virus core protein transforms murine fibroblasts by promoting genomic instability. Cell Oncol. 28 (4), 177–190.
Someya, M., Sakata, K., Matsumoto, Y., Yamamoto, H., Monobe, M., Ikeda, H., Ando, K., Hosoi, Y., Suzuki, N., Hareyama, M., 2006. The association of DNA-dependent protein kinase activity with chromosomal instability and risk of cancer. Carcinogenesis 27 (1), 117–122.
Suwa, A., Hirakata, M., Takeda, Y., Jesch, S.A., Mimori, T., Hardin, J.A., 1994. DNA-dependent protein kinase (Ku protein-p350 complex) assembles on double-stranded DNA. Proc. Natl. Acad. Sci. U.S.A. 91 (15), 6904–6908.
Tanaka, T., Inoue, K., Hayashi, Y., Abe, A., Tsukiyama-Kohara, K., Nuriya, H., Aoki, Y., Kawaguchi, R., Kubota, K., Yoshiba, M., Koike, M., Tanaka, S., Kohara, M., 2004. Virological significance of low-level hepatitis B virus infection in patients with hepatitis C virus associated liver disease. J. Med. Virol. 72 (2), 223–229.
Tsukiyama-Kohara, K., Tone, S., Maruyama, I., Inoue, K., Katsume, A., Nuriya, H., Ohmori, H., Ohkawa, J., Taira, K., Hoshikawa, Y., Shibasaki, F., Reth, M., Minatogawa, Y., Kohara, M., 2004. Activation of the CKI-CDK-Rb-E2F pathway in full genome hepatitis C virus-expressing cells. J. Biol. Chem. 279 (15), 14531–14541.
van Pelt, J.F., Severi, T., Crabbe, T., Eetveldt, A.V., Verslype, C., Roskams, T., Fevery, J., 2004. Expression of hepatitis C virus core protein impairs DNA repair in human hepatoma cells. Cancer Lett. 209 (2), 197–205.
Woo, R.A., McLure, K.G., Lees-Miller, S.P., Rancourt, D.E., Lee, P.W., 1998. DNA-dependent protein kinase acts upstream of p53 in response to DNA damage. Nature 394 (6694), 700–704.
Young, K.C., Lin, P.W., Hsiao, W.C., Chang, T.T., Chang, Y.C., Wu, H.L., 2002. Variation of hepatitis C virus load, hypervariable region 1 quasispecies and CD81 hepatocyte expression in hepatocellular carcinoma and adjacent non-cancerous liver. J. Med. Virol. 68 (2), 188–196.
Zekri, A.R., Sabry, G.M., Bahnassy, A.A., Shalaby, K.A., Abdel-Wahabh, S.A., Zakaria, S., 2005. Mismatch repair genes (hMLH1, hPMS1, hPMS2, GTBP/hMSH6, hMSH2) in the pathogenesis of hepatocellular carcinoma. World J. Gastroenterol. 11 (20), 3020–3026.
Zhang, Y., Riesterer, C., Ayrall, A.M., Sablitzky, F., Littlewood, T.D., Reth, M., 1996. Inducible site-directed recombination in mouse embryonic stem cells. Nucleic Acids Res. 24 (4), 543–548.

GASTROENTEROLOGY 2009;137:285–296

BASIC—LIVER, PANCREAS, AND BILIARY TRACT

Hepatitis C Virus and Disrupted Interferon Signaling Promote Lymphoproliferation via Type II CD95 and Interleukins

KEIGO MACHIDA,[*,‡,§] KYOKO TSUKIYAMA-KOHARA,[*,‖] SATOSHI SEKIGUCH,[*] EIJI SEIKE,[¶] SHIGENOBU TÓNE,[#] YUKIKO HAYASHI,[**] YOSHIMI TOBITA,[*] YURI KASAMA,[‖] MASUMI SHIMIZU,[‡‡] HIDEMI TAKAHASHI,[‡‡] CHYOJI TAYA,[§§] HIROMICHI YONEKAWA,[§§] NOBUYUKI TANAKA,[‡,‖‖] and MICHINORI KOHARA[*]

[*]Department of Microbiology and Cell Biology, Tokyo Metropolitan Institute of Medical Science, Tokyo, Japan; [‡]Department of Immunology, Graduate School of Medicine and Faculty of Medicine, University of Tokyo, Tokyo, Japan; [§]Department of Molecular Microbiology and Immunology, Keck School of Medicine, University of Southern California, Los Angeles, California; [‖]Department of Experimental Phylaxiology, Faculty of Medical and Pharmaceutical Sciences, Kumamoto University, Kumamoto, Japan; [¶]Department of Internal Medicine, Self-Defense Forces Central Hospital, Tokyo, Japan; [#]Department of Biochemistry, Kawasaki Medical School, Okayama, Japan; [**]Department of Pathology, Tokyo Metropolitan Komagome Hospital, Tokyo, Japan; [‡‡]Department of Microbiology and Immunology, Nippon Medical School, Tokyo, Japan; [§§]Laboratory of Animal Science, Tokyo Metropolitan Institute of Medical Science, Tokyo, Japan; and [‖‖]Department of Molecular Oncology, Institute of Gerontology, Nippon Medical School, Kanagawa, Japan

BACKGROUND & AIMS: The molecular mechanisms of lymphoproliferation associated with the disruption of interferon (IFN) signaling and chronic hepatitis C virus (HCV) infection are poorly understood. Lymphomas are extrahepatic manifestations of HCV infection; we sought to clarify the molecular mechanisms of these processes. **METHODS:** We established interferon regulatory factor-1–null (irf-$1^{-/-}$) mice with inducible and persistent expression of HCV structural proteins (irf-1/CN2 mice). All the mice (n = 900) were observed for at least 600 days after Cre/loxP switching. Histologic analyses, as well as analyses of lymphoproliferation, sensitivity to Fas-induced apoptosis, colony formation, and cytokine production, were performed. Proteins associated with these processes were also assessed. **RESULTS:** *Irf-1*/CN2 mice had extremely high incidences of lymphomas and lymphoproliferative disorders and displayed increased mortality. Disruption of *irf-1* reduced the sensitivity to Fas-induced apoptosis and decreased the levels of caspases-3/7 and caspase-9 messenger RNA species and enzymatic activities. Furthermore, the *irf-1*/CN2 mice showed decreased activation of caspases-3/7 and caspase-9 and increased levels of interleukin (IL)-2, IL-10, and Bcl-2, as well as increased Bcl-2 expression, which promoted oncogenic transformation of lymphocytes. IL-2 and IL-10 were induced by the HCV core protein in splenocytes. **CONCLUSIONS: Disruption of IFN signaling resulted in development of lymphoma, indicating that differential signaling occurs in lymphocytes compared with liver. This mouse model, in which HCV expression and disruption of IFN signaling synergize to promote lymphoproliferation, will be an important tool for the development of therapeutic agents that target the lymphoproliferative pathway.**

More than 175 million people worldwide are infected with hepatitis C virus (HCV), which is a positive-strand RNA virus that infects both hepatocytes and peripheral blood mononuclear cells.[1–4] Chronic hepatitis infection can lead to hepatitis, cirrhosis, hepatocellular carcinoma, and lymphoproliferative diseases, such as B-cell non-Hodgkin's lymphomas and mixed cryoglobulinemia.[5–10] The current therapy for chronic HCV infection involves treatment with type I interferon (IFN) and derivatives of IFN, such as pegylated IFN.[11] Treatment with type I IFN is associated with regression of lymphoma in patients with hepatitis C.[12] However, more than 50% of HCV-infected individuals are resistant to treatment, which indicates that the inhibition of IFN signal transduction facilitates the persistent expression of HCV proteins by hepatocytes.

Transgenic mice that express the HCV core protein have been established using a promoter derived from hepatitis B virus,[13] whereas mice that express structural or complete viral proteins have been established using promoters derived from the albumin gene.[14] These mice are immunotolerant to the transgene and do not develop hepatic inflammation, although they do develop age-related hepatic steatosis and hepatocellular carcinomas. We also developed a transgenic mouse model in which the HCV complementary DNA, including viral genes that encode the core, E1, E2, and NS2 proteins, was conditionally expressed by the Cre/*lox*P system (CN2 mice).[15]

Abbreviations used in this paper: IFN, interferon; IL, interleukin; IRF, interferon-regulatory factor; PCR, polymerase chain reaction; WT, wild-type.

0016-5085/09/$36.00
doi:10.1053/j.gastro.2009.03.061

The conditional expression of HCV proteins protected mice from Fas-mediated lethal acute liver failure by inhibiting cytochrome *c* release from the mitochondria.[16] However, the expression of HCV in these mice was usually lost after 21 days. Therefore, an animal model of persistent HCV protein expression is required to examine the effects of chronic HCV infection in vivo.

IFN signaling mediates tumor suppressor effects and antiviral responses and is regulated by key transcription factors of the interferon-regulatory factor (IRF) protein family, including Irf-1, -2, -3, -7, and -9. Targeted disruption of *irf-1* results in aberrant lymphocyte development and a marked reduction in the number of $CD8^+$ T cells in the peripheral blood, spleen, and lymph nodes.[17] In addition, natural killer cell development is impaired in *irf-1*$^{-/-}$ mice.[18] The mechanisms by which HCV infection induces IFN resistance and influences the development of lymphomas are poorly understood. Therefore, in the present study, we established an *irf-1*$^{-/-}$ CN2 mouse model of persistent HCV expression, which allows investigation of the effects of HCV on lymphatic tissue tumor development.

Materials and Methods

Animal Experiments

Wild-type (WT), CN2, *irf-1*$^{-/-}$, and *Mx1-cre* mice were maintained in conventional animal housing under specific pathogen-free conditions. AxCANCre and AxCAw1 were obtained from Dr Izumu Saito (University of Tokyo).[15] To elicit Fas-induced liver damage, adult mice were injected intravenously with 10 μg of purified hamster monoclonal antibody against mouse Fas (clone Jo2; BD Biosciences, San Diego, CA) in 200 μL of phosphate-buffered saline. All animal experiments were performed according to the guidelines of the Tokyo Metropolitan Institute of Medical Science or Kumamoto University Subcommittee for Laboratory Animal Care. The protocol was approved by an institutional review board. Detailed procedures, including induction of the HCV transgene by poly(I:C) in CN2-29 Mx1-Cre mice, are described in Supplementary Materials and Methods.

Measurements of Caspase Activities

The cytosolic splenocyte fractions were isolated as described,[16] and the detailed procedures are described in the Supplementary Material and Methods.

Lentiviral Vectors and Infection

Isolated splenocytes from WT or *irf-1*$^{-/-}$ mice (total of 10^7 cells) were infected with recombinant lentiviruses that express HCV core, E1, E2, NS2, *lacZ*, and empty vector, respectively. One day after infection, cells were selected with puromycin (final concentration of 1 μg/mL). After 5 days of puromycin selection, viable cells were examined.

Baculovirus Expression and Purification of HCV Core, E1, and E2 Proteins

The E1 and E2 sequences from a genotype 1a isolate (strain H77)[19] and a genotype 1b isolate (strain HC-J4),[20] without the C-terminal transmembrane domains but containing the His_6 tag at the C terminus, were cloned into a transfer vector (pBlueBacHis2; Invitrogen, Carlsbad, CA). The expression of recombinant core, E1, and E2 proteins in insect cells and their purification have been described previously.[21]

Results

Viral Protein Expression and Disruption of irf-1 *Synergistically Increase the Development of Lymphoproliferative Disorders*

To clarify the in vivo effects of HCV protein expression, we examined the survival of mice that carry the CN2 transgene (CN2-8, CN2-29).[15] The experimental design is shown in Figure 1*A* (total number of mice, 900). Without Cre/*lox*P switching, the animals that carry the HCV transgene (CN2-8 and CN2-29: core, E1, E2, and NS2 proteins) appeared healthy and developed normally.[15] All of the transgene carriers were observed for at least 600 days after Cre/*lox*P switching (Figure 1*A*). Administration of a recombinant adenovirus that expresses *cre* (AxCANCre) induced the efficient recombination of CN2 transgenes in the hepatocytes from CN2 and *irf-1*$^{-/-}$ CN2 mice (Figure 1*B*). Recombination produced the floxed CN2 transgene (3.3 kilobases) and was completed within 4–7 days; it diminished before day 21 in CN2 mice but persisted in *irf-1*$^{-/-}$ CN2 mice. The expression of core protein in the hepatocytes of CN2 mice peaked on day 7 and decreased to an undetectable level by day 21 (Supplementary Figure 1*A*). The expression of core protein in hepatocytes coincided with a high level of inflammation, as determined by measurements of serum alanine aminotransferase activity (Supplementary Figure 1*A* and data not shown). The HCV core protein was detected in CN2-8 mice 4–14 days after the administration of AxCANCre, and disruption of *irf-1* ensured core protein expression for more than 500 days (Supplementary Figure 1*A* and 1*B*). Therefore, *irf-1* disruption allowed efficient and persistent expression of HCV proteins. HCV core protein gene expression was confirmed by reverse-transcription polymerase chain reaction (PCR) of livers, splenocytes, and peripheral blood monocytes (Supplementary Figure 1*C*). AxCANCre administration to the transgenic mouse induced the efficient expression of HCV transgenes in lymphocytes and splenocytes (Supplementary Figure 1*C*).

The survival rate of WT mice injected with the *cre*-adenovirus (AxCANCre) (Figure 1*C*) or control adenovirus (AxCAw1) (data not shown) was higher than that of the transgenic mice (CN2-8 and CN2-29), which excludes the possibility that the recombinant adenovirus affec-

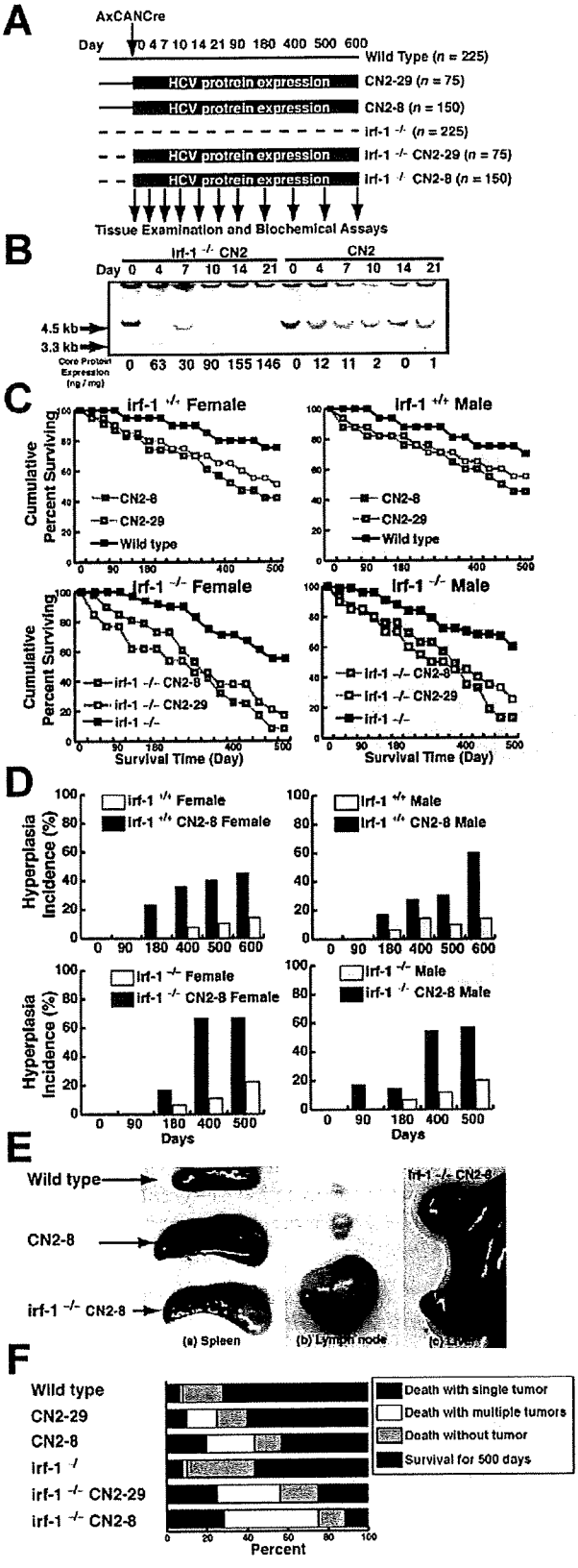

ted the results. More than 75% of the WT mice injected with AxCANCre survived to day 500, whereas the HCV-expressing mice had lower survival rates. The *irf-1*$^{-/-}$ CN2-8 and *irf-1*$^{-/-}$ CN2-29 strains had even lower survival rates, indicating that persistent HCV protein expression in combination with *irf-1* disruption significantly decreases survival (Figure 1*C*).

Lymphoproliferative Disorders Are Accelerated With Age and Level of Viral Protein Expression

To determine the mechanism underlying the increased mortality caused by persistent HCV protein expression in *irf-1*$^{-/-}$ CN2 mice, we examined the kinetics of dysplasia (Figure 1*D*). Strikingly, 67% of the female *irf-1*$^{-/-}$ CN2 mice and 70% of the male *irf-1*$^{-/-}$ CN2 mice developed tumors 400 days after the administration of AxCANCre. Some of the *irf-1*$^{-/-}$ CN2 mice developed hyperplasia of the lymph nodes, and these tumors developed much earlier than the tumors in their *irf-1*$^{+/+}$ or CN2 counterparts (Figure 1*D*). Aberrant cell proliferation developed randomly among the male and female carrier animals between day 180 and day 600. On day 400 after Cre/*lox*P switching, the average weights of the spleens of the WT, CN2, and *irf-1*$^{-/-}$ CN2 mice were 90, 160, and 310 mg, respectively. The disruption of *irf-1* aggravated the HCV-induced spontaneous proliferative disturbances in lymphatic tissues. The number of CN2 mice that died with at least one tumor and the number of tumors per

Figure 1. Disruption of *irf-1* enhances oncogenic potential in combination with HCV transgene expression. (*A*) Experimental design for the animal model. Transgenic mice and their nontransgenic littermates (10–14 weeks of age) were administered the *Cre*-expressing adenovirus (AxCANCre) and killed after 4, 7, 10, 14, 21, 90, 120, 400, 500, or 600 days. (*B*) Southern blot analysis of hepatocyte DNA from mice derived by crossing *irf-1*$^{-/-}$ and HCV-transgenic (CN2) mice. Genomic DNA samples from WT (+/+) and CN2 mouse hepatocytes were digested with *Xba*I and subjected to Southern blot analysis using a radiolabeled genomic flanking probe to determine the rate of recombination of the HCV transgene construct (3.3-kilobase fragment). Disruption of *irf-1* allows persistent expression of HCV proteins. The effects of HCV protein expression on the survival rates of male and female *irf-1*$^{-/-}$ and *irf-1*$^{+/+}$ CN2 mice are shown. (*C*) Kaplan–Meier survival curves for WT mice, *irf-1*$^{-/-}$ mice, CN2 transgenic mouse strains 8 and 29, and *irf-1*$^{-/-}$ CN2-8 and CN-29 mice following infection with a recombinant adenovirus that expresses *cre* (AxCANCre). (*D*) HCV protein expression enhances hyperplasia in male and female CN2 and *irf-1*$^{-/-}$ CN2 mice. The occurrence of hyperplasia was monitored every 7 days for 600 days following the administration of AxCANCre. (*E*) Spleens (*a*) and lymph nodes (*b*) from age-matched WT, CN2, and *irf-1*$^{-/-}$ CN2 mice 500 days after the administration of AxCANCre. (*c*) Liver from the same *irf-1*$^{-/-}$ CN2 mouse (developing severe lymphadenopathy and splenomegaly) following the administration of AxCANCre. (*F*) The cause of death in CN2 transgenic mice with hyperplasias. Mice of each genotype (n = 150) were monitored up to day 600 after the administration of AxCANCre, and necropsies were performed to determine the number of tumors. Tumors included thymomas, splenomas, lymphomas, and hepatocellular carcinomas.

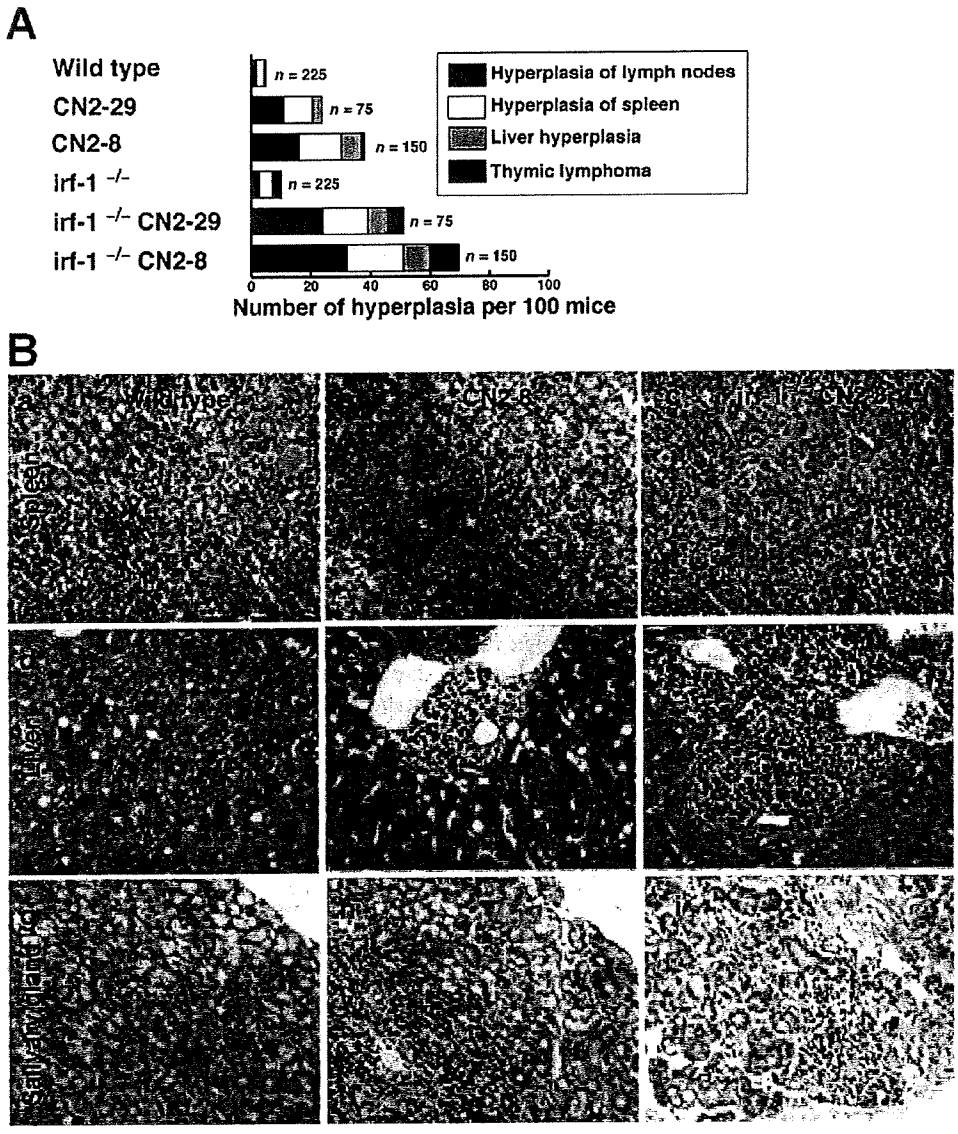

Figure 2. Disruption of *irf-1* aggravates lymphocyte infiltration in combination with HCV transgene expression. (*A*) Histologic analysis of spontaneous proliferative disturbances in the CN2 transgenic mice. Of the 900 mice injected with AxCANCre, 25 of 75 (33%) CN2-29, 47 of 150 (31%) CN2-8, 29 of 75 (39%) *irf-1*$^{-/-}$ CN2-29, and 62 of 150 (41%) *irf-1*$^{-/-}$ CN2-8 mice developed proliferative disturbances. Data shown are from the same cohort of mice analyzed in Figure 1*F*. (*B*) H&E-stained tissue sections of (*a–c*) spleens, (*d–f*) livers, and (*g–i*) salivary glands from age-matched WT, CN2, and *irf-1*$^{-/-}$ CN2 mice after the administration of AxCANCre.

mouse were significantly increased by the ablation of *irf-1* (Figure 1*F*). Although the type of hyperplasia did not differ significantly between the *irf-1*$^{-/-}$ CN2 mice and their *irf-1*$^{+/+}$ CN2 siblings, the time to onset of tumorigenesis differed dramatically (Figure 1*D* and 1*F*), indicating that age is a significant factor in the promotion of lymphomagenesis by HCV proteins.

A significant percentage of the mice that expressed the HCV core protein (*irf-1*$^{-/-}$ CN2 mice) developed polyclonal lymphoid growth disturbances, including splenomegaly, expanded lymph nodes, adenocarcinoma in the abdomen or leg, and lymphoma of the liver or Peyer's patches (Figure 2*A*). In contrast, hepatocytes with abundant expression of HCV proteins rarely developed into hepatocellular carcinomas. H&E staining of splenomegalic tissue revealed extensive hyperplasia of the white pulp zones, in which the cortical zones contained lymphoid follicles and scattered germinal centers, although mitotic figures were rarely observed (Figure 2*B* and data not shown). These results indicate that persistent expression of HCV proteins frequently induces lymphoproliferative disorders in addition to liver hyperplasia, which is consistent with the phenotype of patients with hepatocellular carcinoma.[3,4,9]

Abnormal T-Cell and B-Cell Proliferation in HCV Transgenic Mice

To characterize the disruption of lymphocyte proliferation due to HCV protein expression in the transgenic mice, we used flow cytometry to determine the ratio of T cells to B cells by staining with antibodies directed against CD3, CD45R, CD4, CD8, and the T-cell receptor. The average ratio of T cells to B cells in the lymph nodes and spleens of CN2 mice was significantly higher than

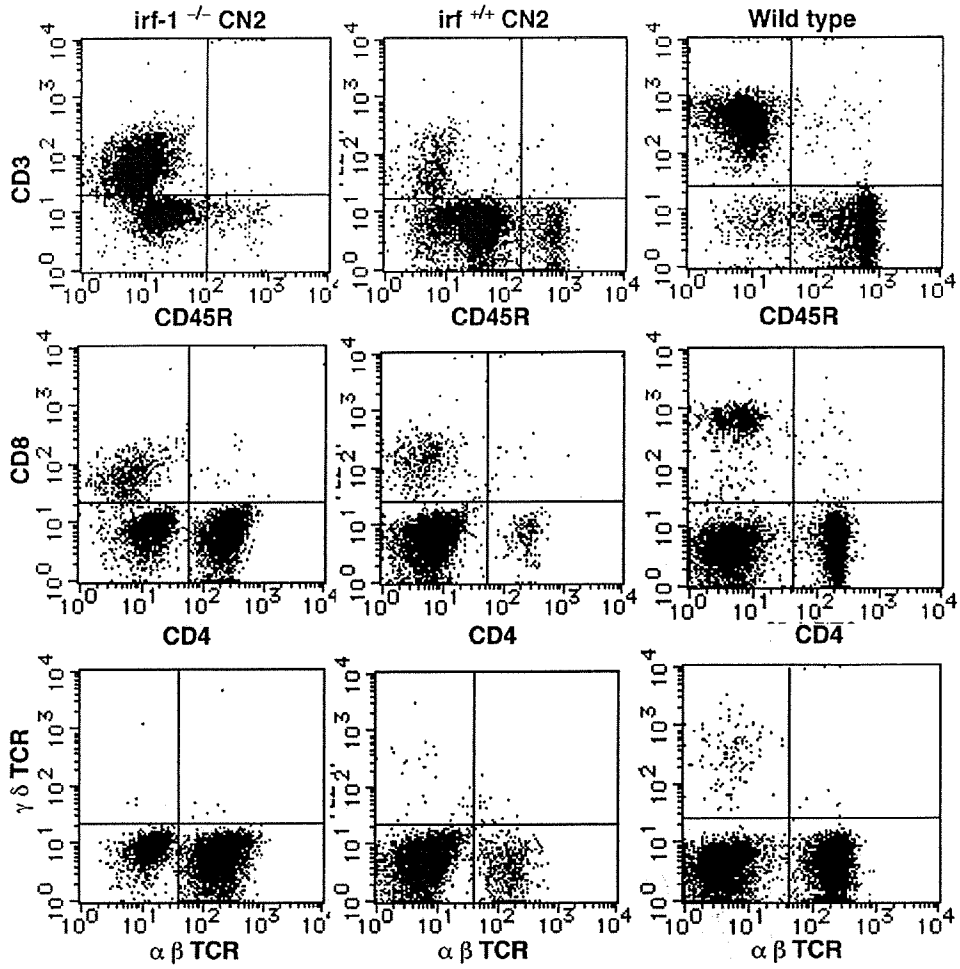

Figure 3. HCV expression and *irf-1* ablation affect the lymphocyte population. T-cell and B-cell proliferation in *irf-1*$^{+/+}$ CN2 mice, *irf-1*$^{-/-}$ CN2 mice, and WT mice. CD3$^+$, CD45R$^+$, CD4$^+$, CD8$^+$, and T-cell receptor–positive cells from age-matched *irf-1*$^{-/-}$ CN2, *irf-1*$^{+/+}$ CN2, and WT mice with hyperplasia were analyzed by fluorescence-activated cell sorting. Lymphocytes were prepared from CN2-8 and WT littermates at the age of 16 months, after administration of AxCANCre for 400 days.

that in the WT mice. The majority of the CD3$^+$ lymphocytes and a few CD8$^+$ lymphocytes expressed CD4 on their surfaces. The proliferating cells were mainly CD4$^+$ T cells, although some were CD45R$^+$B cells (Figure 3 and data not shown). The *irf-1*$^{-/-}$ CN2 mice also developed B-cell lymphomas (data not shown). These results confirm that HCV protein expression induces lymphoproliferative disorders that involve excessive expansion of both T and B cells. In *irf-1*$^{-/-}$ CN2 mice, the cell population that was negative for T-cell receptor (α, β, γ, and δ isoforms) staining was smaller than that in the other mice.

Inhibition of Fas-Induced Apoptosis Owing to Disruption of irf-1 *Leads to Persistent Expression of HCV in Transgenic Mouse Livers*

The Fas ligand is essential for the development of hepatitis via cytotoxic T-lymphocyte–mediated cell killing.[22] Therefore, we determined the sensitivities of *irf-1*$^{-/-}$ hepatocytes to Fas-induced apoptosis. The *irf-1*$^{-/-}$ mice and WT littermates were injected intravenously with a monoclonal antibody against Fas. The disruption of *irf-1* inhibited Fas-induced apoptosis, presumably by decreasing the levels of caspase-6 and -7 messenger RNA (mRNA; Supplementary Figure 2). These results suggest that the reduced expression of effector caspases delays Fas-mediated apoptosis in *irf-1*$^{-/-}$ mice and abrogates the elimination of HCV-expressing cells in vivo.

Stable Expression of HCV Proteins Induces Lymphoproliferative Diseases

To confirm that HCV proteins induce lymphoproliferation without the adenoviral vector system, switching of the expression of HCV proteins was conducted using the Mx promoter–driven cre recombinase with poly(I:C) induction (Figure 4*A*). The Mx promoter is active in hepatocytes as well as in hematopoietic cells. We crossed CN2 mice with Mx1-Cre transgenic mice; CRE recombinase was expressed from the IFN-inducible *Mx1* promoter. Injection of the Mx1-Cre/CN2-29 mice with poly (I:C) induced IFN production and efficiently induced the generation of CN2 gene products in hematopoietic cells

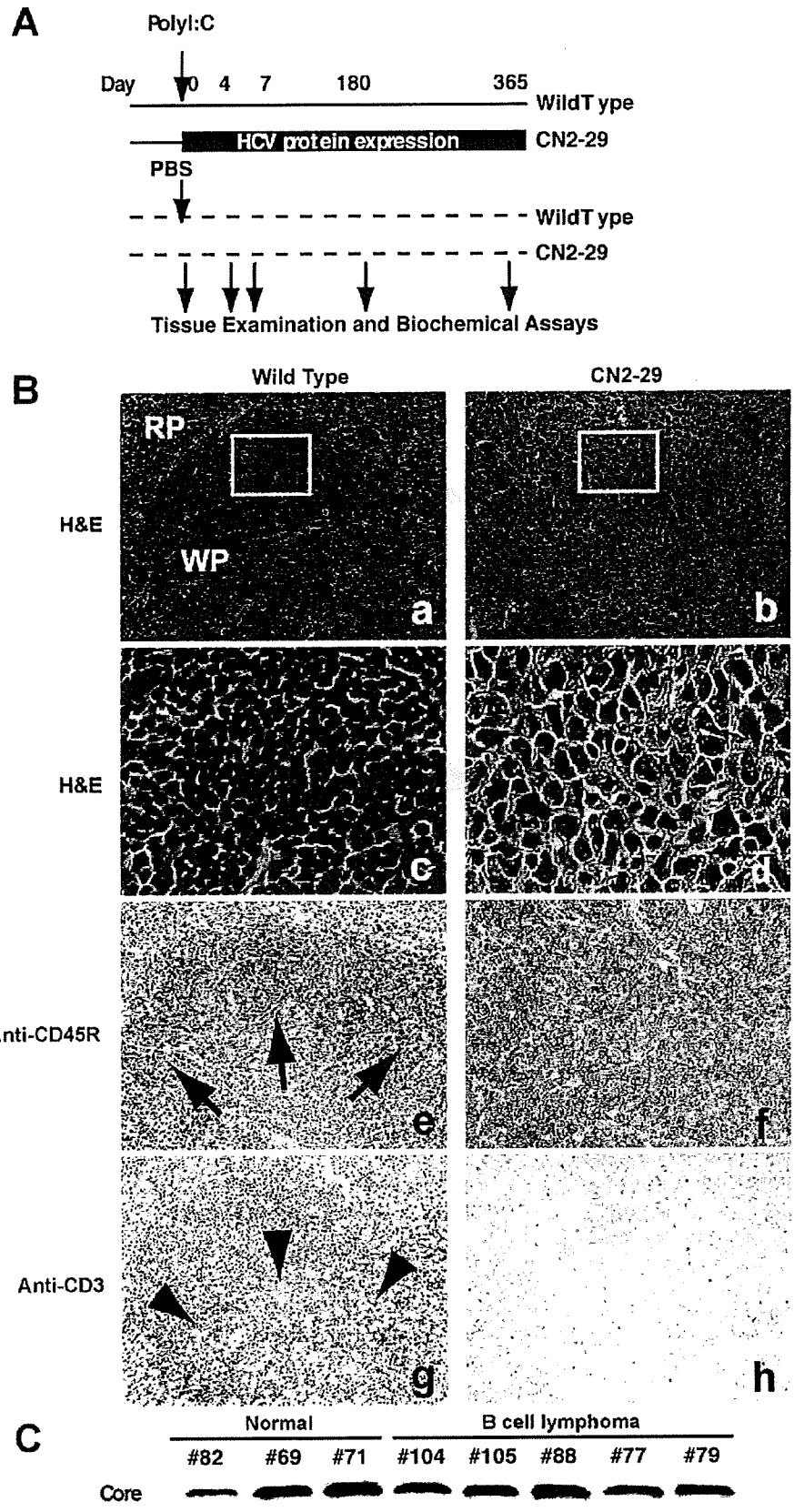

Figure 4. Stable expression of HCV viral proteins induces lymphoproliferative diseases. (*A*) Switching of the expression of HCV proteins was conducted using the Mx promoter–driven cre recombinase with poly(I:C) induction. The Mx promoter is active in hepatocytes as well as in hematopoietic cells. We crossed CN2 mice with Mx1-Cre transgenic mice; Cre recombinase was expressed from the IFN-inducible *Mx1* promoter. Injection of Mx1-Cre/CN2-29 mice with poly(I:C) induces IFN production and efficiently induces the expression of CN2 gene products in hematopoietic cells (mainly in Kupffer cells and lymphocytes), livers, and spleens but not in most other tissues. (*B*) The white pulp (WP) and red pulp (RP) comprise the components of the spleen in WT mice. The neoplastic cells replace the normal structures, such as the white pulp and red pulp. (*c* and *d*) The neoplastic cells are larger than lymphocytes (*c*), and the nuclei are irregular, round, oval, elongated, and polygonal (*d*). (*e* and *g*) The white pulp in WT mice consists of both a B-cell–rich area (*arrows*, *e*) and T-cell–rich area (*arrowheads*, *g*). (*f* and *h*) The neoplastic cells show staining for the B-cell marker CD45R, thereby supporting the diagnosis of B-cell lymphoma (*f*), while they do not show staining for the T-cell marker CD3 (*h*). *Frames c* and *d* are higher-magnification views of the white box areas in *a* and *b*, respectively. (*C*) Core protein expression was confirmed by immunoblotting.

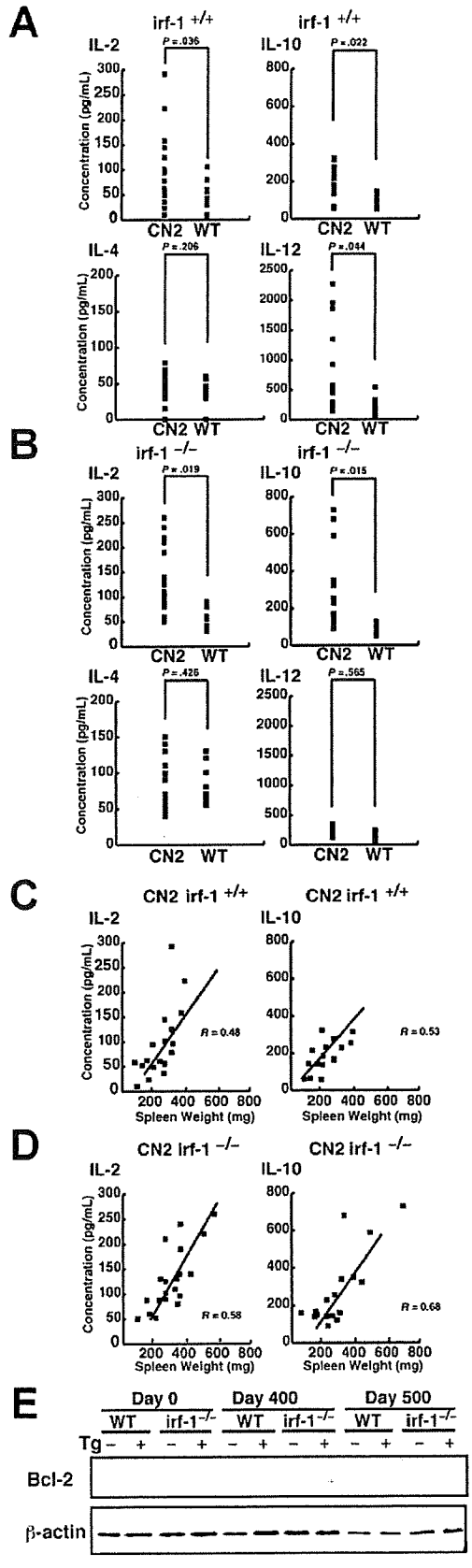

(mainly in Kupffer cells and lymphocytes), liver, and spleen but not in most other tissues. At 7 days after induction of viral proteins, HCV core proteins were detected in both hepatocytes and hematopoietic cells (data not shown). After 180 days, almost 40% of the CN2(-29) mice developed lymphomas, whereas the WT mice did not (Figure 4*B*). The neoplastic cells were larger than lymphocytes, and their nuclei were irregular, round, oval, elongated, and polygonal. HCV core protein expression was confirmed by immunoblotting (Figure 4C), and increases in the levels of interleukin (IL)-2, IL-10, and IL-12 were observed (data not shown). The hematopoietic marker CD45R was detected in the lymphoproliferative regions and spleens (Figure 4*B*). The efficiency of expression switching was confirmed by both the HCV transgene copy numbers and protein expression using quantitative PCR and immunoblotting, respectively (Supplementary Figure 3). These results further validate that sustained expression of HCV proteins induces lymphoproliferation.

Increased IL-2, IL-10, and IL-12 Levels in HCV Transgenic Mice

To study the mechanisms of HCV-induced lymphoproliferative diseases, we measured the serum IL-2, IL-4, IL-10, and IL-12 levels in the CN2 transgenic mice and their WT littermates (Figure 5*A*). The serum IL-4 concentration did not differ significantly between the CN2 and WT mice following injection with AxCANCre. However, the CN2 mice had significantly increased levels of serum IL-2, IL-10, and IL-12. Notably, the CN2 mice with proliferative disturbances in the lymph nodes and spleen had dramatically elevated levels of these cytokines, suggesting that altered cytokine production is involved in aberrant lymphocyte proliferation or differentiation in CN2 mice. In contrast, the *irf-1*$^{-/-}$ CN2 mice did not show elevated levels of serum IL-12 but had significantly higher levels of serum IL-2 and IL-10 compared with *irf-1*$^{-/-}$ mice (Figure 5*B*). Thus, the disruption of *irf-1* abrogates the increase in IL-12 level but augments the increases in the levels of IL-2 and IL-10 in CN2 mice. These results indicate that IL-2 and IL-10 play key roles

Figure 5. HCV protein expression alters the cytokine profile. (*A*) The serum IL-2, IL-4, IL-10, and IL-12 levels in *irf-1*$^{+/+}$ CN2 (Tg+) and *irf-1*$^{+/+}$ WT mice were measured by enzyme-linked immunosorbent assay. (*B*) The serum IL-2, IL-4, IL-10, and IL-12 levels in *irf-1*$^{-/-}$ CN2 (Tg+) and *irf-1*$^{-/-}$ WT mice were measured by enzyme-linked immunosorbent assay. The *P* values are based on comparisons of the mean cytokine concentrations. (*C* and *D*) Relationship between the IL-2 or IL-10 concentration in the serum and the spleen weights of (*C*) CN2irf-1$^{+/+}$ or (*D*) CN2irf1$^{-/-}$ mice with progressive lymphoproliferation. The numbers of points in the graphs correspond to the numbers of tested animals. (*E*) Bcl-2 protein levels in the lymph nodes of *irf-1*$^{+/+}$ (WT) and *irf-1*$^{-/-}$ transgenic (CN2) (Tg+) and WT mice on days 0, 400, and 500 after the administration of AxCANCre. Bcl-2 migrates at 26 kilodaltons. β-Actin was used as a loading control.

in the induction of the lymphoproliferative phenotype in *irf-1*$^{-/-}$ CN2 mice.

To verify the relationship between the weights of the lymph organs and the cytokine levels, the correlation coefficients were calculated according to Pearson (Figure 5*C* and 5*D*). Whereas spleen weight did not markedly influence the increase in IL-4 level (data not shown), a significant positive correlation was found between spleen weight and increased IL-2 and IL-10 levels in CN2 gene-expressing mice on the *irf-1*$^{-/-}$ background ($R = 0.58$, $P < .05$, and $R = 0.68$, $P < .05$, respectively) (Figure 5*D*). With respect to the serum levels of IL-2 and IL-10, a less intensive but significant positive correlation was found between the cytokine levels and spleen weights of CN2 gene-expressing mice on the *irf-1*$^{+/+}$ background ($R = 0.43$, $P < .05$, and $R = 0.53$, $P < .05$, respectively) (Figure 5*C*). These results indicate that IL-2 and IL-10 are involved in lymphoproliferation in viral protein-expressing mice.

Aberrant Expression of Bcl-2 in Expanded Lymph Nodes of CN2 Mice

Bcl-2 immunoglobulin transgenic mice develop follicular lymphoproliferation[23] due to the inability of various stimuli to induce apoptosis in these mice.[24] Therefore, to examine whether HCV causes dysregulation of Bcl-2 in lymphoid tissues, we examined the expression of Bcl-2 (Figure 5*E*). Lymph nodes collected from *irf-1*$^{-/-}$ CN2 mice 400 days after the administration of AxCANCre showed elevated levels of Bcl-2. Immunoblot analysis revealed that a doublet for Bcl-2 (26 and 28 kilodaltons) appeared in some samples 500 days after AxCANCre administration, suggesting the presence of phosphorylated and nonphosphorylated Bcl-2.[25]

Combination Cytokine Treatment Enhances Splenocyte Colony Formation in Synergy With Viral Protein Expression

To determine whether aberrant cytokine profiles contribute to lymphocyte transformation, a colony formation assay was performed using the methylcellulose method. Mouse splenocytes were infected with adenoviruses that expressed the *cre* DNA recombinase or *lacZ* control. Expression of HCV core proteins was induced by cre-adenovirus infection of the splenocytes (Figure 6*A*). Colony counting was performed at postinfection day 28 (Figure 6*B*). Combined treatment with IL-2 and IL-10 greatly enhanced colony formation, especially in the splenocytes of HCV transgenic mice (CN2-29, *irf-1*$^{-/-}$ CN2-29). The addition of IL-12 suppressed colony formation induced by combined treatment with IL-2 and IL-10. In the *irf-1*$^{-/-}$ background, treatment with IL-2 plus IL-10 or IL-2 plus IL-12 greatly enhanced colony formation. To determine whether enhanced colony formation correlated with cytokine-induced Bcl-2 expression, the Bcl-2 mRNA levels in the splenocytes were quantified (Figure 6*C*). Because IL-2 enhances T-lymphocyte proliferation and transformation,[26] it is of particular interest that treatment with IL-2 plus IL-10 resulted in marked increases in both lymphocyte transformation and the Bcl-2 mRNA levels upon HCV transgene expression. These results indicate that dysregulated cytokine expression, disruption of *irf-1*, and HCV transgene expression synergistically enhance splenocyte transformation.

Cytokine Treatment and HCV Transgene Expression Synergistically Inhibit Fas-Mediated Apoptosis

To determine whether cytokines inhibit Fas-induced apoptosis, we treated the splenocytes from transgenic and WT mice with cytokines and then measured Fas-induced apoptosis by Annexin V staining and fluorescence-activated cell sorting, and we also assayed caspase enzymatic activity (Figure 6*D* and 6*E*). IL-10 treatment in the presence of IL-2 greatly inhibited Fas-induced apoptosis. Furthermore, *irf-1* disruption made the splenocytes resistant to Fas-induced apoptosis in the presence of IL-2, IL-10, and/or IL-12. In particular, IL-2 plus IL-10 treatment produced the strongest inhibition of Fas-induced apoptosis. These cytokines also up-regulated the Bcl-2 mRNA levels in splenocytes, which indicates that IL-2, IL-10, and/or IL-12 up-regulate *bcl-2* expression, which subsequently inhibits Fas-induced apoptosis. This result is consistent with reports that IL-10 and/or IL-2 treatment induce *bcl-2* in B or T lymphocytes.[10,27] Caspase-3/7 activity was correlated with the level of *bcl-2* expression (Figure 6*C* and 6*F*). These results indicate that aberrant cytokine expression and disruption of IFN signaling affect *bcl-2* expression, which is associated with the inhibition of caspase expression.

HCV Core and E2 Proteins Mediate IL-2, IL-10, and IL-12 Expression

To determine which viral protein is responsible for cytokine expression, individual viral proteins were stably expressed in splenocytes using recombinant lentiviruses that express the HCV core, E1, E2, NS2, and lacZ. Each gene expression profile was confirmed by reverse-transcription PCR (Supplementary Figure 4). Only the HCV core protein induced IL-2 and IL-10 (Figure 7*A*). To determine whether extracellular viral proteins trigger cytokine expression, recombinant viral proteins were added to the cells. Only the viral envelope protein E2 induced IL-12 (Figure 7*B*). These results indicate that the HCV core and E2 proteins are responsible for IL-2, IL-10, and IL-12 expression.

HCV Core and IL-10 Induce Bcl-2 Expression

To determine whether viral protein expression and cytokine stimulation synergistically induce Bcl-2 expression, individual viral proteins were stably expressed using lentiviral vectors, and the cells were tested for Bcl-2 expression. Core protein expression and IL-10 stimula-

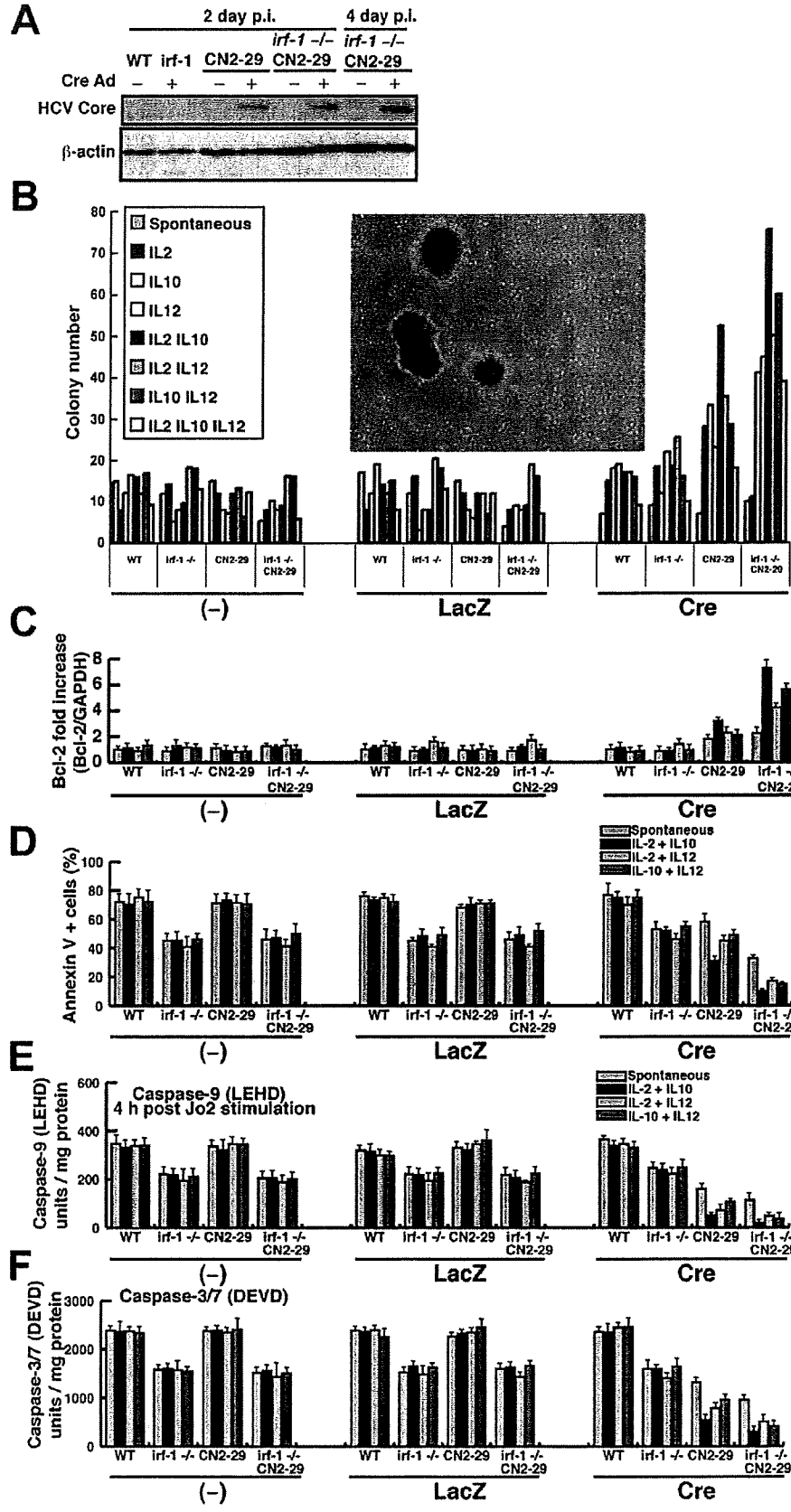

Figure 6. Lymphocyte transformation by aberrant cytokines and inhibition of apoptotic signaling. (*A*) Expression of the HCV core protein (21 kilodaltons) in *irf-1*$^{+/+}$ (WT) and *irf-1*$^{-/-}$ transgenic (CN2-29) and WT mice 2 or 4 days postinfection (p.i.) with AxCANCre (multiplicity of infection, 1.0). β-Actin was used as a loading control. (*B*) Colony formation assay for splenocytes from *irf-1*$^{+/+}$ (WT) and *irf-1*$^{-/-}$ WT or transgenic (CN2-29) mice in the absence or presence of the indicated cytokine and infected with mock, LacZ, and Cre adenoviruses. The *inset* shows an image of the colonies generated from the *irf-1*$^{-/-}$ CN2 splenocytes (original magnification 10×). (*C*) Quantification, by quantitative reverse-transcription PCR of Bcl-2 mRNA relative to control glyceraldehyde-3-phosphate dehydrogenase mRNA in the splenocytes of *irf-1*$^{+/+}$ (WT) and *irf-1*$^{-/-}$ or transgenic (CN2-29) mice treated with the indicated cytokines and infected with mock, LacZ, and cre adenoviruses. (*D*) Apoptosis measured by Annexin V fluorescence-activated cell sorting analysis of splenocytes from *irf-1*$^{+/+}$ (WT) and *irf-1*$^{-/-}$ or transgenic (CN2-29) mice treated with the indicated cytokines and infected with the mock, LacZ, and cre adenoviruses. (*E* and *F*) The caspase-9 and caspase-3/7 enzymatic activities in splenocytes from *irf-1*$^{+/+}$ (WT) and *irf-1*$^{-/-}$ or transgenic (CN2-29) mice treated with the indicated cytokines were measured using a substrate cleavage assay after infection with the mock, LacZ, and Cre adenoviruses. Caspase-9 activity was measured 4 hours after injection of the anti-Fas monoclonal antibody (Jo2). LEHD, substrate for caspase-9; DEVD, substrate for caspase-3/7. Vertical bars are SD and were determined using the Student *t* test.

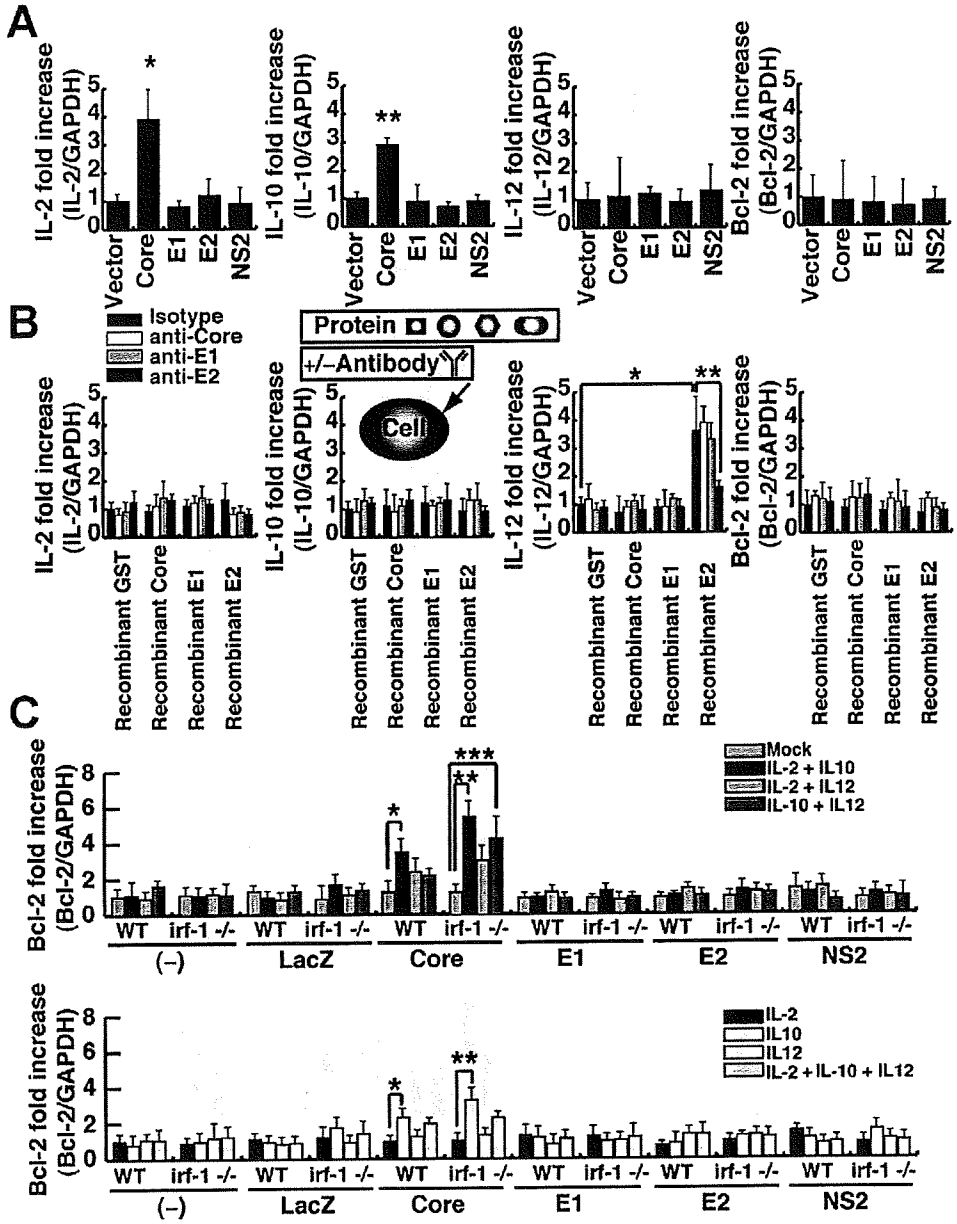

Figure 7. Induction of IL-2 and IL-10 by HCV core and IL-12 by E2 and of Bcl-2 by HCV core plus cytokines. (*A*) Individual viral proteins were stably expressed in splenocytes using recombinant lentiviruses that expressed the HCV core, E1, E2, NS2, and lacZ. Each gene expression profile was determined by quantitative reverse-transcription PCR. (*B*) E2 binding induces IL-12 in Raji cells, as determined by quantitative reverse-transcription PCR. Cells were treated with HCV core, E1, E2 (genotypes 1a and 1b), or glutathione *S*-transferase proteins, and the cytokine and bcl2 cellular RNA levels were examined using quantitative reverse-transcription PCR. (*C*) Quantification by quantitative reverse-transcription PCR of Bcl-2 mRNA relative to control glyceraldehyde-3-phosphate dehydrogenase mRNAin splenocytes from *irf-1*$^{+/+}$ (WT) and *irf-1*$^{-/-}$ WT or Irf-1$^{-/-}$ mice treated with the indicated cytokines and infected with lentiviruses that express mock, core, E1, E2, NS2, and LacZ. Individual viral proteins were stably expressed using lentiviral vectors, and the cells were tested for Bcl-2 expression.

tion induced Bcl-2, while the other proteins did not (Figure 7*C*). Interestingly, the combination of IL-2 and IL-12 only induced Bcl-2 in the *irf-1*$^{-/-}$ background, while triple stimulation (IL-2, IL-10, and IL-12) did not induce Bcl-2 (Figure 7*C*). These results indicate that complex signaling networks induce Bcl-2 in the presence of viral nucleocapsid proteins.

Discussion

The present study shows that Bcl-2 levels, cytokine levels, aging, and inflammation enhance the development of lymphoproliferative disorders caused by HCV proteins (Supplementary Figure 5). Disruption of *irf-1* enables the persistent expression of HCV protein, leading to lymphoproliferative diseases owing to reduced apoptosis (ie, lower levels of caspase-1, -6, and -7 expression). HCV CN2 transgenic (Tg+) mice are resistant to Fas-induced apoptosis due to the inhibition of cytochrome *c* release from mitochondria.[16] Mice with disruption of *irf-1* have several defects of their innate and adaptive immunity, such as lineage-specific defects in thymocyte development; immature T cells can develop into mature CD4$^+$ cells but not into CD8$^+$ T cells.[18,28] IRF-1 controls the positive and negative selection of CD8$^+$ thymocytes.[29] IRF-1 is required for the development of the Th1-type immune response, and

its absence leads to the induction of the Th2-type immune response.[18,30] Because the number of natural killer cells is dramatically reduced in *irf-1*$^{-/-}$ mice,[18] this defect may cause the marked increase in viral protein expression and the inhibition of tumor surveillance mechanisms, leading to the development of non-Hodgkin's lymphoma. Expression of the IL-12 p40 subunit is defective in *irf-1*$^{-/-}$ mice.[18]

Lymphomagenesis may require the additional genetic instability provided by HCV-induced hypermutation (2-hit model). Important questions are raised regarding the lymphoproliferative mechanisms of lymphomas in HCV-infected patients (B-cell malignancies predominate). Hypermutation of the immunoglobulin genes in B cells induced by HCV infection is the cause of the lymphomagenesis seen in HCV infection,[21,31] and this model may provide more direct insights into lymphoma production, because HCV-induced hypermutation causes genetic instability and causes chromosomal aberrations, possibly resulting in neoplastic transformation.[32] In addition, the antiapoptotic phenotype generated by sustained viral protein expression may enhance the survival of lymphocytes and inhibit activation-induced cell death to turn off the activated lymphocytes. The dysregulated cytokine profiles and sustained lymphocyte survival may alter the fates of regulatory T cells and dendritic cells.[33]

In conclusion, the present study shows that the conditional expression of HCV proteins induces inflammation and lymphoproliferative disorders, which are enhanced by *irf-1* disruption. Therefore, IRF-1–inducible genes probably play essential roles in suppressing HCV-induced lymphoma and in eliminating HCV protein-expressing cells. Our transgenic mice provide evidence that the overexpression of apoptosis-related proteins, including Bcl-2, and/or aberrant cytokine production are primary events in HCV-induced lymphoproliferation. It is interesting to note that lymphoproliferation was dominant over liver tumor development in the present study. Approximately 40% of the CN2-29Mx1Cre mice developed B-cell lymphomas, while 5% of the mice developed liver tumors. Further molecular analyses will enlighten the differential signaling pathways between hepatocytes and lymphocytes and increase our understanding of the differences between lymphomagenesis and liver tumor development caused by HCV.

Supplementary Data

Note: To access the supplementary material accompanying this article, visit the online version of *Gastroenterology* at www.gastrojournal.org, and at doi: 10.1053/j.gastro.2009.03.061.

References

1. Saito I, Miyamura T, Ohbayashi A, et al. Hepatitis C virus infection is associated with the development of hepatocellular carcinoma. Proc Natl Acad Sci U S A 1990;87:6547–6549.
2. Simonetti RG, Camma C, Fiorello F, et al. Hepatitis C virus infection as a risk factor for hepatocellular carcinoma in patients with cirrhosis. A case-control study. Ann Intern Med 1992;116: 97–102.
3. Ferri C, Monti M, La Civita L, et al. Infection of peripheral blood mononuclear cells by hepatitis C virus in mixed cryoglobulinemia. Blood 1993;82:3701–3704.
4. Silvestri F, Pipan C, Barillari G, et al. Prevalence of hepatitis C virus infection in patients with lymphoproliferative disorders. Blood 1996;87:4296–4301.
5. Rui L, Goodnow CC. Lymphoma and the control of B cell growth and differentiation. Curr Mol Med 2006;6:291–308.
6. Dietrich CF, Lee JH, Herrmann G, et al. Enlargement of perihepatic lymph nodes in relation to liver histology and viremia in patients with chronic hepatitis C. Hepatology 1997;26:467–472.
7. Ascoli V, Lo Coco F, Artini M, et al. Extranodal lymphomas associated with hepatitis C virus infection. Am J Clin Pathol 1998; 109:600–609.
8. De Vita S, De Re V, Sansonno D, et al. Gastric mucosa as an additional extrahepatic localization of hepatitis C virus: viral detection in gastric low-grade lymphoma associated with autoimmune disease and in chronic gastritis. Hepatology 2000;31: 182–189.
9. Mele A, Pulsoni A, Bianco E, et al. Hepatitis C virus and B-cell non-Hodgkin lymphomas: an Italian multicenter case-control study. Blood 2003;102:996–999.
10. Cohen SB, Crawley JB, Kahan MC, et al. Interleukin-10 rescues T cells from apoptotic cell death: association with an upregulation of Bcl-2. Immunology 1997;92:1–5.
11. Pawlotsky JM. The nature of interferon-alpha resistance in hepatitis C virus infection. Curr Opin Infect Dis 2003;16:587–592.
12. Levine AM, Shimodaira S, Lai MM. Treatment of HCV-related mantle-cell lymphoma with ribavirin and pegylated interferon alfa. N Engl J Med 2003;349:2078–2079.
13. Moriya K, Fujie H, Shintani Y, et al. The core protein of hepatitis C virus induces hepatocellular carcinoma in transgenic mice. Nat Med 1998;4:1065–1067.
14. Lerat H, Honda M, Beard MR, et al. Steatosis and liver cancer in transgenic mice expressing the structural and nonstructural proteins of hepatitis C virus. Gastroenterology 2002;122:352–365.
15. Wakita T, Taya C, Katsume A, et al. Efficient conditional transgene expression in hepatitis C virus cDNA transgenic mice mediated by the Cre/loxP system. J Biol Chem 1998;273:9001–9006.
16. Machida K, Tsukiyama-Kohara K, Seike E, et al. Inhibition of cytochrome c release in Fas-mediated signaling pathway in transgenic mice induced to express hepatitis C viral proteins. J Biol Chem 2001;276:12140–12146.
17. Yokota T, Oritani K, Takahashi I, et al. Adiponectin, a new member of the family of soluble defense collagens, negatively regulates the growth of myelomonocytic progenitors and the functions of macrophages. Blood 2000;96:1723–1732.
18. Taki S, Sato T, Ogasawara K, et al. Multistage regulation of Th1-type immune responses by the transcription factor IRF-1. Immunity 1997;6:673–679.
19. Yanagi M, Purcell RH, Emerson SU, et al. Transcripts from a single full-length cDNA clone of hepatitis C virus are infectious when directly transfected into the liver of a chimpanzee. Proc Natl Acad Sci U S A 1997;94:8738–8743.
20. Yanagi M, St Claire M, Shapiro M, et al. Transcripts of a chimeric cDNA clone of hepatitis C virus genotype 1b are infectious in vivo. Virology 1998;244:161–172.
21. Machida K, Cheng KT, Pavio N, et al. Hepatitis C virus E2-CD81 interaction induces hypermutation of the immunoglobulin gene in B cells. J Virol 2005;79:8079–8089.

22. Kondo Y, Sung VM, Machida K, et al. Hepatitis C virus infects T cells and affects interferon-gamma signaling in T cell lines. Virology 2007;361:161–173.
23. McDonnell TJ, Deane N, Platt FM, et al. bcl-2-immunoglobulin transgenic mice demonstrate extended B cell survival and follicular lymphoproliferation. Cell 1989;57:79–88.
24. Lacronique V, Mignon A, Fabre M, et al. Bcl-2 protects from lethal hepatic apoptosis induced by an anti-Fas antibody in mice. Nat Med 1996;2:80–86.
25. Ito T, Deng X, Carr B, et al. Bcl-2 phosphorylation required for anti-apoptosis function. J Biol Chem 1997;272:11671–11673.
26. Stem JB, Smith KA. Interleukin-2 induction of T-cell G1 progression and c-myb expression. Science 1986;233:203–206.
27. Levy Y, Brouet JC. Interleukin-10 prevents spontaneous death of germinal center B cells by induction of the bcl-2 protein. J Clin Invest 1994;93:424–428.
28. Taniguchi T, Ogasawara K, Takaoka A, et al. IRF family of transcription factors as regulators of host defense. Annu Rev Immunol 2001;19:623–655.
29. Penninger JM, Sirard C, Mittrucker HW, et al. The interferon regulatory transcription factor IRF-1 controls positive and negative selection of CD8+ thymocytes. Immunity 1997;7:243–254.
30. Lohoff M, Ferrick D, Mittrucker HW, et al. Interferon regulatory factor-1 is required for a T helper 1 immune response in vivo. Immunity 1997;6:681–689.
31. Machida K, Cheng KT, Sung VM, et al. Hepatitis C virus induces a mutator phenotype: enhanced mutations of immunoglobulin and protooncogenes. Proc Natl Acad Sci U S A 2004;101:4262–4267.
32. Machida K, Kondo Y, Huang JY, et al. Hepatitis C virus (HCV)-induced immunoglobulin hypermutation reduces the affinity and neutralizing activities of antibodies against HCV envelope protein. J Virol 2008;82:6711–6720.
33. Dolganiuc A, Paek E, Kodys K, et al. Myeloid dendritic cells of patients with chronic HCV infection induce proliferation of regulatory T lymphocytes. Gastroenterology 2008;135:2119–2127.

Received June 25, 2008. Accepted March 31, 2009.

Reprint requests

Address requests for reprints to: Michinori Kohara, PhD, Department of Microbiology and Cell Biology, Tokyo Metropolitan Institute of Medical Science, 3-18-22 Honkomagome, Bunkyo-ku, Tokyo 113-8613, Japan. e-mail: mkohara@rinshoken.or.jp; fax: (81) 3-3828-8945.

Acknowledgments

The authors thank Prof Tadatsugu Taniguchi for his scholarly support of this study; Kazuaki Inoue and Kentaro Tomita for their advice on histology; Yutaka Amako, Isao Maruyama, and Kohsuke Tanaka for technical assistance; and Mitsugu Takahashi for breeding the transgenic mice.

Conflicts of interest

The authors disclose no conflicts.

Funding

Supported in part by a research fellowship from the Japan Society for the Promotion of Science; a grant from the Ministry of Education, Culture, Sports, Science and Technology of Japan; a grant from the Ministry of Health, Labour and Welfare of Japan; and the Program for Promotion of Fundamental Studies in Health Sciences of the National Institute of Biomedical Innovation of Japan. This project was also supported by National Institutes of Health research grants P50AA11999, 5P30DK048522-13, and CA108302.

Available online at www.sciencedirect.com
ScienceDirect
Comparative Immunology, Microbiology and Infectious Diseases 32 (2009) 29–41
COMPARATIVE IMMUNOLOGY MICROBIOLOGY & INFECTIOUS DISEASES
www.elsevier.com/locate/cimid

Inhibition of host protein synthesis in B95a cells infected with the HL strain of measles virus

Yoshihisa Inoue [a], Kyoko Tsukiyama-Kohara [b], Misako Yoneda [a], Hiroki Sato [a], Chieko Kai [a,*]

[a] *Laboratory Animal Research Center, The Institute of Medical Science, The University of Tokyo, 4-6-1 Shirokanedai Minato-ku, Tokyo 108-8639, Japan*
[b] *Department of Experimental Phylaxiology, Faculty of Medical and Pharmaceutical Sciences, Kumamoto University, 1-1-1 Honjo Kumamoto, Kumamoto 860-8556, Japan*

Accepted 9 August 2008

Abstract

The shut-off of host protein synthesis in virus-infected cells is one of the important mechanisms for viral replication. In this report, we showed that the HL strain of measles virus (MeV-HL) as well as other field isolates, which were isolated from human blood lymphocytes using B95a cells, induce the shut-off in B95a cells. Since the Edmonston strain of MeV failed to induce the shut-off in B95a cells, the ability to induce the shut-off was considered to be dependent on virus strains. Although, the modification of eukaryotic translation initiation factors (eIF) including eIF4G, eIF4E, and 4E-BP1 was reported for shut-off by various viruses, the involvement of these eIFs was not observed in MeV-HL-infected B95a cells. Instead, the accumulation of phosphorylated eIF2α was found to coincide to the decrease of host protein synthesis, suggesting the involvement of phosphorylation of eIF2α in inhibition of translation as one of the mechanisms of the shut-off.

Keywords: Measles virus; Shut-off; eIF2α

Résumé

La suppression de la synthèse protéique de la cellule hôte au cours de l'infection est un des mécanismes majeurs de la réplication virale. Dans cette étude nous avons montré que la souche HL du virus de la rougeole (MeV-HL) ainsi que d'autres souches sauvages du virus, isolées dans

* Corresponding author. Tel.: +81 3 5449 5497; fax: +81 3 5449 5379.
E-mail address: ckai@ims.u-tokyo.ac.jp (C. Kai).

0147-9571/$ – see front matter © 2008 Elsevier Ltd. All rights reserved.
doi:10.1016/j.cimid.2008.08.007

des cellules B95a à partir de lymphocytes sanguins humains, induisent ce type de suppression dans les cellules B95a. Comme la souche Edmonston du virus de la rougeole est incapable d'induire cette suppression dans les cellules B95a, cette propriété a été considérée comme dépendante de la souche virale. Bien qu'il ait été observé une extinction de l'expression des facteurs d'initiation de la traduction eucaryote (eIF) dont eIF4G, eIF4E et 4E-BP1 par de nombreux virus, il n'a pas été vu d'implication de ces facteurs dans les cellules B95a infectées par MeV-HL. Par contre, dans ces cellules on a montré que l'accumulation de la forme phosphorylée de eIF2a est concomitante à la diminution de la synthèse protéique, suggérant l'inhibition de la traduction par phosphorylation de eIF2a dans pourrait être un des mécanismes de la suppression de la synthèse protéique.

Mots clés : virus de la rougeole ; eIF2α ; suppression de la synthèse protéique

1. Introduction

One of the most striking changes observed in the cells infected with certain viruses is the almost complete inhibition of the translation of host mRNAs in the presence of effective translation of viral mRNAs [1]. Such inhibition of host protein synthesis (shut-off) have been reported in the infection with picornaviruses, adenovirus, influenza virus and vesicular stomatitis virus (VSV) and considered to occur at the stage of host translational level, as cellular mRNAs are recovered as an intact and functionally active form from the virus-infected cells [2–5]. Modification of eukaryotic initiation factors (eIFs) including the subunit of eIF4F complex (e.g., eIF4G and eIF4E) is observed in these virus-infected cells [6], and the modification of eIF4F by the viral infection resulting in the inhibition of cap-dependent translation is proposed as one of the mechanisms for shut-off.

Measles virus (MeV) belongs to the genus *Morbillivirus* within the family Paramyxoviridae, the genome of which is a single-stranded RNA with negative polarity. The MeV mRNA has a cap structure at 5′ end of the mRNA and is thought to be translated in a cap-dependent manner [7]. The Edmonston strain of MeV (MeV-Ed) has been reported not to induce the host shut-off of host protein synthesis [8,9]. Although most information on MeV–cell interaction has been obtained from the studies on MeV-Ed in epithelial or epithelial-like cells such as CV-1, Hela and Vero cells, accumulating evidence obtained by the use of lymphoblastoid B95a cells has suggested that MeV circulating in human is heterogenous and MeV-Ed represent minor subpopulation of the virus selected during long passage in cell cultures [10].

In the present study, we examined the effect of the HL strain of MeV (MeV-HL), which was isolated using B95a cells from a measles patient and maintains virulence in monkeys [10], on the host protein synthesis in B95a cells and found that MeV-HL induces marked shut-off of host protein synthesis. As the mRNA level of host proteins was not altered in MeV-HL-infected B95a cells, we focused on possible modification of translation factors involved in the cap-dependent translation initiation to clarify the mechanisms involved in the induction of the shut-off of host protein synthesis by MeV-HL infection.

2. Materials and methods

2.1. Cell and viruses

B95a cells [11] were grown in RPMI1640 supplemented with 5% fetal calf serum (FCS). As a typical virus isolated from measles patient, MeV-HL and two other field isolates, 9106 and 9301 strains [12] were used. MeV-Ed that was passed twice in B95a cells was also used. Virus infectivity titers were determined in B95a cells and expressed as a 50% tissue culture infectious dose ($TCID_{50}$). For examining shut-off of host protein synthesis, a monolayer culture of B95a cells was infected with MeV with a multiplicity of infection (MOI) of 1 $TCID_{50}$.

2.2. Metabolic labeling of cells

B95a cells were mock-infected or infected with MeV and then labeled with [^{35}S] EXPRESS (PerkinElmer, MA, USA) in methionine- and cystein-free RPMI1640 with 2% FCS for 1 h at 0, 11, 17, 23 and 35 h post-infection (hpi). Cells were lysed in lysis buffer C (125 mM NaCl, 20 mM Tris–HCl pH 8.0, 0.5% NP-40). Cell lysates were centrifuged and the supernatants were collected. Proteins were electrophoresed in SDS-PAGE gels, and ^{35}S-labeled proteins were visualized with autoradiography using X-ray film or quantitated with a phosphoimager plate in BAS 2000 (Fujifilm, Tokyo, Japan).

2.3. Real-time RT-PCR

Real-time RT-PCR was used to determine the expression level of glyceraldehyde-3-phosphate dehydrogenase (GAPDH) mRNA and 18S rRNA in accordance with the method described by Sato et al. [13].

2.4. Antibodies

Rabbit polyclonal antibodies against eIF4G and eIF2α, goat polyclonal antibodies against phospho-eIF4E, 4E-BP1 and β-actin and mouse monoclonal antibody against eIF4E were purchased from Santa Cruz Biotechnology, Inc. (CA, USA). Rabbit polyclonal antibody against phospho-eIF2α was purchased from Cell Signaling Technology (MA, USA). Horseradish peroxidase-conjugated secondary antibodies against rabbit, goat or mouse immunoglobulin were purchased from DAKO (Glostrup, Denmark).

2.5. Western blotting assay

Mock- or MeV-HL-infected B95a cells were lysed with lysis buffer C containing 1 mM PMSF, 1 mM benzamidine, 1 μg/ml aprotinine, 100 μM NaF and 1 μM Na_3VO_4. Equal amounts of protein extracts were subjected to SDS-PAGE and the proteins were transferred onto Hybond-N(+) nitrocellulose membrane (GE Healthcare UK Ltd., Buckinghamshire, UK). Detection of 4E-BP1 was performed as described previously [14]. Western blotting assay was performed with each antibody according to the recommendations of

manufacturer. Bands were visualized using an ECL plus detection reagent (GE Healthcare UK Ltd.). The intensity of bands was quantitated by scanning with LAS-1000 mini and Imagegauge software (Fujifilm).

2.6. Establishment of cell lines stably expressing eIF2α

Human eIF2α cDNA was obtained with PCR using the sense primer (5′-GCGGGAATCACACACATACCTCAGAA-3′) and antisense primer (5′-TCAAGTCTAG-GATTTACAGCCAGGAAGCGC-3′) with reverse transcription (RT) products from the mRNA of HeLa cells and was then subcloned into pCR2.1-TOPO vector (Invitrogen, CA, USA). Phosphorylation site at serine 51 of eIF2α cDNA was mutated to alanine (S51A) using a PCR-based mutagenesis strategy with Pfu turbo polymerase (Stratagene, CA, USA) to obtain the cDNA of S51A mutant eIF2α. The eIF2α cDNA was inserted into a pCMV-myc expressing vector (Clontech, CA, USA). The myc-tagged eIF2α (wild type or S51A mutant) expression vector (1.5 μg) and 0.5 μg of pCDNA3.1 (Invitrogen) were co-transfected to B95a cells with DMRIE-C reagent (Invitrogen) according to the recommendations of manufacturer. After incubation for 24 h, the cells were replated to 150-mm dishes and cultured in RPMI1640 with 5% FCS and 500 μg/ml G418 (bioactive; Invitrogen). G418-resistant colonies were selected approximately 2 weeks later. Expression of myc-tagged proteins was confirmed by Western blotting assay using a monoclonal antibody against myc tag (Clontech).

3. Results

3.1. Effect of several strains of MeV on host protein synthesis in B95a cells

Effect of MeV-HL-infection on protein synthesis was shown in Fig. 1a. The rate of host protein synthesis was determined by quantitation of the total radioactivity of one lane except four bands of N, P, M and H derived from MeV-HL. The ratio of host protein synthesis in MeV-HL-infected B95a cells to that in mock-infected cells was shown in Fig. 1b. The relative rate of viral protein synthesis to host protein synthesis, which was determined by sum of the radioactivity of four viral proteins and that of host proteins, was also shown in Fig. 1b. A marked decrease of host protein synthesis was observed between 18 and 36 hpi. On the other hand, relative viral protein synthesis to host protein synthesis increased and reached a peak at 24 hpi. This result indicates that MeV-HL induces shut-off of host protein synthesis in B95a cells.

Subsequently, other field isolates of MeV, 9106 strain and 9301 strain were also examined for their ability to induce the shut-off (Fig. 2a right). The autoradiograph gel was stained with Coomassie brilliant blue before drying the gel to confirm that total protein levels are equal (Fig. 2a left). As shown in Fig. 2a, 9106 and 9301 strains also induced the inhibition of host protein synthesis at 24 hpi similar to MeV-HL. The effect of the MeV-Ed, which was reported not to induce shut-off in CV-1 or Hela cells, was tested in B95a cells. Host protein synthesis in MeV-Ed-infected B95a cells was not inhibited until 24 hpi when the inhibition was clearly observed in MeV-HL-infected cells (Fig. 2b). These results

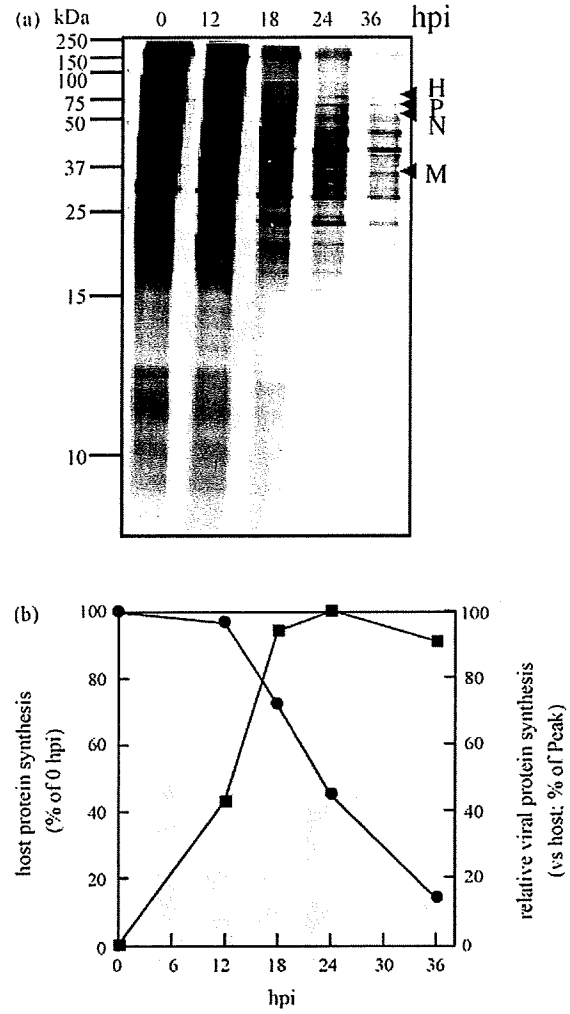

Fig. 1. Protein synthesis in B95a cells infected with MeV-HL. (a) B95a cells infected with MeV-HL were labeled with a mixture of [^{35}S] methionine/cysteine for 1 h and collected at the indicated time. Labeled proteins were separated by 12% SDS-PAGE gel. The proteins derived from MeV-HL are indicated to the right of the image. (b) Quantitation of host protein synthesis (closed circle) and relative viral protein synthesis to host protein synthesis (closed square). The rates of protein synthesis were determined from images as described in the text.

indicate that field isolated MeVs, which maintain their virulence, have an ability to induce shut-off of host protein synthesis, whereas only the MeV-Ed does not.

3.2. *Effect of MeV-HL infection on GAPDH mRNA*

The expression level of the GAPDH gene, one of house keeping genes, was measured as a representative to determine whether MeV-HL-induced inhibition of host protein synthesis occurs at the transcription stage (Fig. 3). The relative expression level of GAPDH